Flake like Copper Oxide Nanostructures and their Application in Electrocatalytic Sensing of Growth-Promoting Agents

Nizamuddin Solangi[1], Sorath Solangi[1], Gul Naz[2,*] iD, Ghulam Murtaza Mastoi[1,3]

A compact and intimate interfacial contact between the modified film and the conducting electrode is crucial for electrochemical biosensors. The direct drop-casting of nanomaterials onto the working electrode often fails to construct a compact interfacial arrangement, which results in sluggish electrode kinetics. Here, we describe a simple and cost-effective strategy to produce CuO nanostructure using a modified hydrothermal route. The in-situ growth allowed the formation of a highly ordered interconnected network of sharp flakes configured in the form of large spheres with excellent ITO surface coverage. The CuO nanostructures were highly electrochemically active toward the oxidation of β–adrenergic agonists, i.e., formoterol fumarate (FF). The analytical ability was studied by comparison of the electrochemical behavior of ITO based electrode with its glassy carbon electrode counterpart. The binder-less CuO-based ITO electrode successfully determined FF with a detection window of 0.01 µM to 0.46 µM with practical application for real broiler feed samples collected from the local poultry farms in Hyderabad, Pakistan.

Introduction

The increasing food demand, particularly the growing consumption of meat-based products, has fostered the illicit and unchecked use of growth-promoting chemicals in cattle feed. The -adrenergic agonists, such as formoterol fumarate, are of particular interest, responsible for enhancing the nutrient flow from fat to muscle in livestock, are widely abused in countries such as Pakistan and India, Bangladesh and China [1]. The illegitimate use of FF in livestock feed to facilitate meat production has been linked with several human health-related issues, including muscle tremors, confusion, cardiac palpitation and nervousness [2]. Thus, the quantification of FF in complex matrices such as biological samples and livestock products is an important issue regarding food process monitoring and quality control. The traditional approach toward the quantification of FF includes the application of techniques such as LC-MS [3], UV-spectrophotometry [4], HPLC [5] and GC [6]. Despite their great accuracy and selectivity, these approaches have several drawbacks, including lengthy sample preparation processes, high analytical costs, and time-consuming procedures. [7]. On the other hand, electrochemical technologies promise to downsize and allow for the fabrication of sensor systems capable of transforming the analysis from the lab to the field [8]. Although FF is an electro-active molecule, its electrochemical characteristics are less known. In this regard, Demircigil, B., *et. al.,* [9] investigated the behaviour of FF over conventional GCE. However, the sluggish electrode response resulted in low-signal sensitivity and a narrow quantification range, which was unsuitable for practical applications.

The integration of nanomaterials as electrode modifiers has proven significant to overcome such restraints. The inherent surface area of nanomaterials and the high electro-catalytic activity can effectively facilitate the electron-transfer kinetics, enabling high electrode signal sensitivity [10]. Gan, T., *et. al.,* (2016) [11] demonstrated the potential application of copper oxide@silica oxide spheres as the effective electrode material to determine FF in swine feed samples.

The drop-casting or overlaying of nanomaterials over the electrode surface is reported to be the most suitable way of integrating nanomaterials with a conventional electrode system. Despite their effectiveness, these slurry-derived electrode devices have major flaws such as uneven distribution and lumping (aggregation) of nanomaterials on

[1]Institute of Advanced Research Studies in Chemical Sciences (IARSCS), University of Sindh, Jamshoro 76080, Pakistan
[2]Department of Chemistry, Beijing Key Laboratory for Microanalytical Methods and Instrumentation, Key Laboratory of Bioorganic Phosphorus Chemistry and Chemical Biology, Tsinghua University, Beijing 100084 (P. R. China)
[3]Dr. M.A Kazi Institute of Chemistry University of Sindh Jamshoro, Sindh 76080, Pakistan

*Corresponding author:
E-mail: gls19@mails.tsinghua.edu.cn; Tel.: + 92 333-2761963

Advanced Materials Letters
https://aml.iaamonline.org

IAAM®
International Association of
Advanced Materials
www.iaamonline.org

the collector surface. The use of Nafion® and chitosan for substrate-modifier adhesion invigorates these issues and questions the overall performance of electrodes [12]. Since these issues stem from off-substrate nanomaterial synthesis, an alternative approach allows in-situ generation of nanostructures on electrode surfaces, increases the electrode-modifier contact area and improves control of morphology, surface coverage, and distribution/ arrangement of nanostructures on electrode surfaces is required [13]. Thus, in contrast to its conventional slurry-derived counterpart, the working electrode constructed through an in-situ process results in a binder-free electrode with significant simplicity and reliability [14,15]. However, control of the growth process is one of the major problems, particularly in the case of metal oxide, wherein heat-assisted growth spawns over-sized structures having negligible adherence to the electrode surface. Thus, in the perpetuation of our recent work [16], the current study deals with the in-situ growth of CuO nanostructures over ITO substrate to produce a working electrode sensitive to the determination of FF. Here, oxalic acid (dicarboxylic acid) was used as a growth direction and regulating agent in the hydrothermal synthesis of the CuO structures. The newly developed electrode exhibited excellent electro-catalytic potential against electro-oxidation of FF in aqueous solution. Moreover, the study provides sufficient evidence for higher sensitivity, utmost reproducibility and enduring capability of the devised electrode when referenced against conventional slurry-based GCE electrode. In addition, the selective quantification of FF from boiler feed samples garnered from various poultry farms situated in the vicinity of Hyderabad region, served as a practical recognition of devised electrode.

Experiments

Chemicals

The study used analytical grade materials including copper chloride ($CuCl_2 \cdot 2H_2O$) from Shandong Fousi Chemical Co., Ltd. Oxalic acid ($C_2H_2O_4$) and reagents like ammonia solution (NH_3) (37%) were purchased from Hebei Iverson Biotechnology Co., Ltd. The formoterol fumarate dehydrates ($C_{23}H_{30}N_2O_9$) were obtained from Pharmachem (Wuhan) International Co., Ltd. Nafion® (1.7%) ($C_7HF_{13}O_5S.C_2F_4$) (Sigma) dissolved in isopropanol (C_3H_8O) (Merk) was used as the active binder for the slurry-based electrode. Britton-Robinson buffer (BRB) was used as an electrolyte.

Growth of copper oxide (CuO) nanoflowers

A simple hydrothermal process was used to grow CuO nanostructures onto an ITO substrate. A 1.7g of $CuCl_2.5H_2O$ was mixed with 1.0g of oxalic acid in 100 mL of deionised water. Once the solution reached complete homogenization, a pre-cleaned ITO substrate (1×1 cm^2) was allowed to sit in the bed of the container with its conductive side facing upwards. To begin the growing

process, 4.5 ml of 37% NH_3 was added to the container, and then aluminium foil was put onto the container. The container was hydrothermally treated at a temperature of 85 °C for about 6 h. After the reaction, ITO substrates were removed and washed thoroughly with deionised first and then methanol alternatively to annihilate any surface-bound contaminants.

Characterization

The CuO nanostructures were assessed for their morphological and structural characteristics using high-resolution scanning electron microscopy (HR-SEM) (JSM-7001F) and x-ray diffraction (XRD) (Bruker D-8). The FT-ATR (Nicolet 5700 Thermo) spectra were recorded for standard oxalic acid and assisted CuO-based ITO electrodes. The electrochemical measurements were carried out using CHI 760E electrochemical workstation (CH instrument Texas, USA) housed with a three-electrode system. The Ag/AgCl served as reference and platinum wire as a counter electrode in a characteristic electrochemical experiment.

Preparation of slurry-based GCE

The powder-version of the same CuO nanostructures was used to modify the glassy carbon electrode using a simple drop-casting approach. Before surface modification, the GCE was extensively polished and ultrasonically cleaned in deionised water. The surface modification was achieved by drop-casting 5 µL of CuO suspension (0.15 mg in 10 mL methanol). The electrode was then allowed to dry, and the surface was coated with 1 µL Nafion® solution (1.7 %).

The preparation of real sample (broiler feed)

To demonstrate the practical workability of the sensor system, GCE-CuO NS was investigated to determine FF from the broiler feed samples collected from the local poultry farms within the vicinity of the Hyderabad region, Pakistan. The standard addition method was used to confirm the quantification [11]. A 2 g of broiler feed sample was introduced with different concentrations of FF (0.15 to 0.35 µM) in addition to 10 mL of ethyl acetate. This mixture was stirred for 5 min followed by high-speed centrifugation (6000 RPMs) for 10 min. The BRB buffer was used to dilute the collected supernatant before further testing.

Results and discussion

Fig. 1 shows the FE-SEM images of CuO nanostructures. As seen, the as-synthesised CuO nanostructures have adopted sphere–like morphological features composed of sharp flake-like structures (**Fig. 1(b-c)**). Such small nano-structural units are responsible for enhancing the selectivity and response rate of the sensor system based on increased surface permeability and grain interfaces. Moreover, the consistency in structural features and morphological uniformity of the nanostructures is evident, indicating complete and uniform material growth.
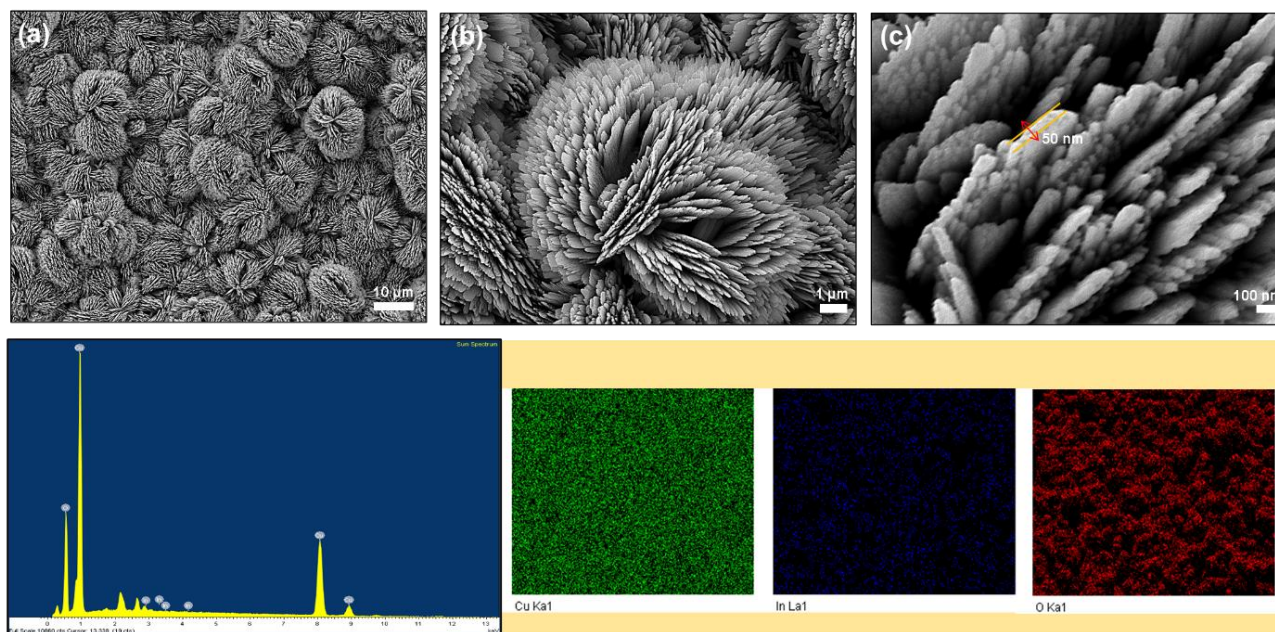
Fig. 1. FE-SEM images for copper oxide nanostructures with flake-like structural features and (a-c); the corresponding EDS spectrum and elemental mapping confirming the presence of Cu, O as primary elements and In from ITO substrate.
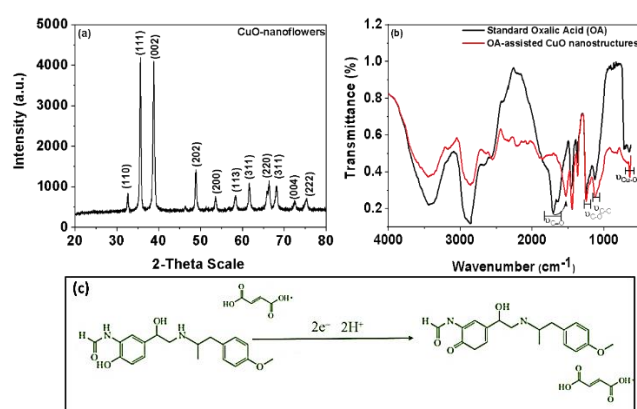
Fig. 2. XRD pattern and (a); FTIR spectra of copper oxide nanoflowers (c) the electrochemical oxidation mechanism of FF.

The regular distribution of nanostructures over the ITO substrate with negligible structural collapse signifies the robustness of the in-situ grown nanostructures. The average thickness of the spike-like structure was estimated in the range of 20 to 50 nm, with 5 to 10 nm calculated for the small surface residing thorns. The EDS analysis further confirms the compositional purity of CuO nanostructures with Cu, and O as major elements and in as secondary elements from the ITO substrate. The XRD pattern (**Fig. 2(a)**) consisting of peaks indexed to (110) (111) (002) (212) (113) (220) (311) (004), and (222) further reflects the formation of monoclinic CuO phase as supported by ICCD Card No45-0937 [17]. The FTIR spectra confirm the interaction of oxalic acid with CuO (**Fig. 2(b)**). In the case of dicarboxylic acids, the steric arrangement could enable the interaction of carbonyl groups with CuO, leaving the free moiety to act as surface-bound functionality at the nanostructure-solvent interface or to interact with adjacent CuO nanoparticles. These interactions would lead to a shift in the carbonyl vibrational frequencies [18]. The typical band of oxalic acid is identified at 1710 cm^{-1}. The band associated with oxalic acid's C–O and C–C bond can be seen at 1257 and 1123 cm^{-1}, respectively. The metal-carboxylates can be found in the range of 1650–1510 and 1400–1280 cm^{-1} for the symmetrical and asymmetrical vibrations, respectively [19]. A shift from 1710 to 1520 cm^{-1} is evident in the case of oxalic acid-assisted CuO indicating the uni-dentate binding nature of oxalic acid at the surface of CuO nanostructures. Moreover, a well-built metal-oxide band near 600 cm^{-1} is indicative of CuO.

As mentioned earlier, the growth of CuO nanostructures was achieved within an aqueous pre-cursor mixture comprised of metal salt, ammonia and oxalic acid. In the absence of an active driving force for material deposition, the precipitation is anticipated to be sedated and steered, which is crucial for obtaining uniform growth over a solid substrate. In this case, the OH – ions released from ammonia are responsible for metal hydroxide precipitation over the conductive substrate. The homogenous generation of OH – throughout the mixture enhances the uniformity of the formed nanostructures. The presence of oxalic acid further reduces this precipitation process, allowing the directed growth of CuO. The growth mechanism may be ascribed through the following equations:

$$Cu^{+2} + 4NH_3 \rightarrow [Cu(NH_3)_4]^{+2} \qquad \text{(i)}$$

$$[Cu(NH_3)_4]^{+2} + 2OH^- \rightarrow Cu(OH)_2 + NH_4OH \qquad \text{(ii)}$$

$$Cu(OH)_2 \rightarrow CuO + H_2O \qquad \text{(iii)}$$

Advanced Materials Letters
https://aml.iaamonline.org

IAAM®
International Association of
Advanced Materials
www.iaamonline.org
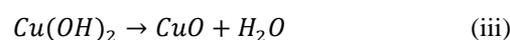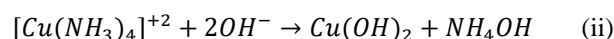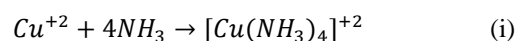
Contrary to other metal oxides, CuO readily changes $Cu(OH)_2$ (orthorhombic) into CuO at 85°C without the need for further calcination at high temperatures (monoclinic). Moreover, the provision of ITO substrate as support for in-situ growth also curtails the surface effects, consequently resulting in precise nanomaterial characteristic properties of CuO [20].

The electrochemical assessment was carried out using 0.01 µM FF solution within 0.1 BRB buffer (pH 6.0). **Fig. 3** shows the CV curves measured for ITO-CuO NS with bare ITO and GCE. The bare ITO generated no notable response, whereas the bare GCE produced a large anodic peak at 0.35 V. Unlike bare GCE, ITO-CuO NS exhibited a robust redox repose at a much lower-over potential value of 0.22 V with superior current density (**Fig. 3(a)**). The high current response with low-over potential value in the case of ITO-CuO NS is a synergetic enhancement observed because of excellent, efficient surface architectures and engineering that results from in-situ growth of CuO over ITO substrate. The electrochemical response of GCE modified with a powdered version of a CuO was also assessed. The variance in electrochemical signal may be attributed to the electrode modification technique, which is more efficient than the drop-casting method, as the surface architecture of nanostructures used in GCE and ITO are identical. The electron transfer rate was further estimated from the charge transfer co-efficient (α) values obtained from the Tafel slope measured for ITO-CuO NS and GCE-CuO NS. The identified value of 0.68 for ITO-CuO NS is higher than 0.57 noted for GCE-CuO NS, suggesting the enhanced electron-transfer kinetics favorability over ITO-CuO NS. Further, the substantially excessive surface area with unabridged coverage of CuO nanostructures grown in-situ enables escalated charge transportation undermining the congestion propounded by the binder.

The exact electrochemical oxidation mechanism for FF is still debatable. However, due to its structural resemblance with phenolic derivatives, oxidation of FF via hydroxyl moieties associated with aromatic rings has been postulated by Demircigil, B. T., *et. al.,* (2002) [21] (**Fig. 2(c)**). In this case, the oxidation of FF is achieved via an active Cu(I)/Cu(II) redox couple. Cu (II) is produced in the anodic sweep, causing electro-oxidation of a surface bounded FF molecules generating electrons responsible for the noted anodic peak (**Fig. 3(a)**). The reverse sweep then enables regeneration of Cu(I) through the de-oxidation of Cu(II), enabling the material to detect FF from an aqueous solution actively.

Since the electro-oxidation of FF is a diffusion-controlled process, chronoamperometric measurements were carried out to determine the diffusion coefficient (D) using a revised form of the Cottrell equation against 0.1 to 0.4 mM concentration of FF [22].

$$I = nFAD^{1/2}C_b\pi^{-1/2}t^{-1/2} \qquad (1)$$

$$D = \left(\frac{m}{nFAC_b\pi^{-\frac{1}{2}}}\right)^2 \qquad (2)$$
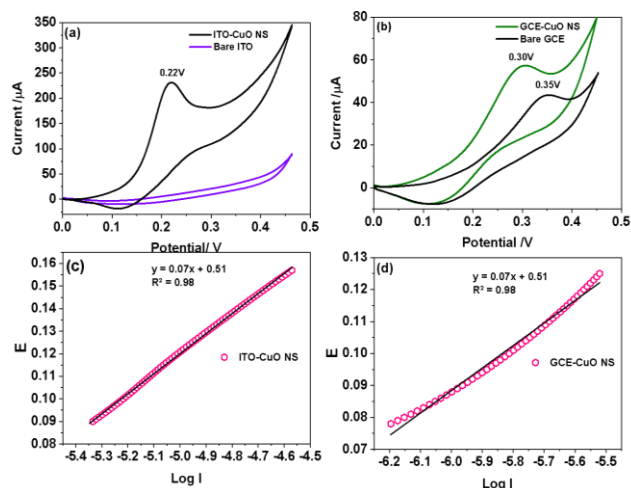
Fig. 3. CV profile of bare and ITO-based CuO nanostructures compared to (b) powdered version of CuO in standard 0.01 µM FF solution, and their (c-d) corresponding Tafel slopes justifying higher charge-transfer kinetics for CuO nanoflowers.

Besides the usual meaning of n, F and π, C_b represents the concentration of FF while A denotes the area of the ITO electrode. **Fig. 4(a)** shows the I v.s $t^{-1/2}$ plot, where the corresponding slopes are then plotted against the concentration of FF. The final slope values estimate D using equation (2). The D value for ITO-CuO NS was calculated as 2.99×10^{-5} cm²/s. The rate constant (k) was obtained using a modified form of the Galus equation:

$$\frac{I_c}{I_L} = \gamma^{1/2}\pi^{1/2} = \pi^{\frac{1}{2}}(k_hC_bt)^{1/2} \qquad (3)$$

The Ic is the current response of ITO-CuO NS for FF, whereas I_L denotes the amount of limiting current without FF. The terms k_h, C_b and t are catalytic constant, the concentration of FF and the elapsed time. The graph of Ic/I_L v.s $t^{1/2}$ from the chronoamperometric measurements is shown as an inset in **Fig. 4(a)**, where the average K_h was determined to be 2.71×10^3 mol^{-1}Ls^{-1}.

The estimated value is evident of the well-endowed electron transportation abilities of in-situ grown CuO nanostructures, suggesting its feasibility as an alternative to the slurry-derived electrodes.

Diffusion voltammetry (DPV) measured FF in the 0.01 µM to 0.46 µM. The DPV profile is presented in **Fig. 4(b)**, with **Fig. 4(c)** depicting the corresponding calibration curve. The detection limit (LOD) and quantification (LOQ) were estimated as 1×10^{-3} and 0.09 µM.
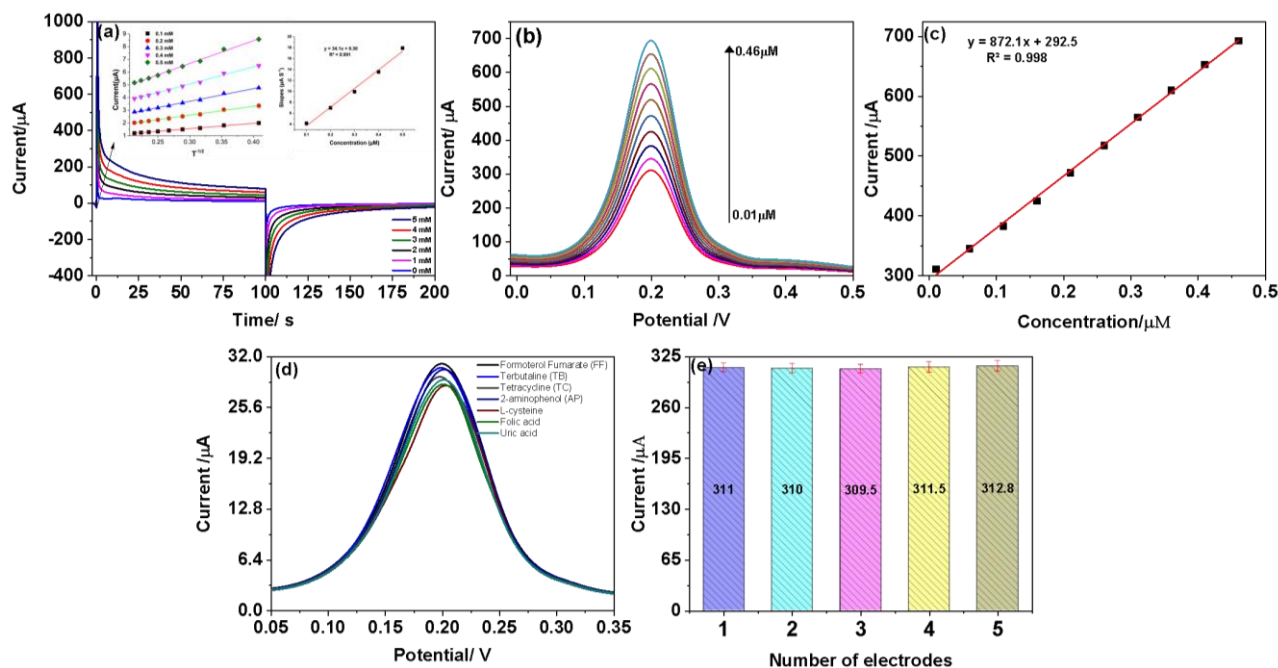
Fig. 4. The chronoamperometric measurements (a) and the DPV profile with a corresponding calibration curve for different FF concentrations (b-c), the DPV response for CuO nanoflowers in the presence of various interferents (d) and the bar-graph representing a variation of current density with different number of CuO-based electrodes fashioned similarly to assess repeatability.

Table 1. Comparison of ITO-CuO NS based electrochemical sensor with other sensor system utilising conventional modification approach.

Type of Electrode	Modification method	Modifier	Performance		Measured Potential (V)	Reference
			LOD (µM)	Linear Range (µM)		
GCE	-----	----	35.4	0.6 to 8.0	0.78	[9]
GCE	Drop-casting	copper oxide@silica oxide spheres	0.005	0.03 to 10	0.45	[11]
GCE	Drop-casting	CuO NF	0.01	0.1 to 5	0.4	[12]
ITO	*In-situ*	*CuO nano-spikes*	*0.001*	*0.01 to 0.46*	*0.22*	*This work*

The selectivity of the electrode was assessed in the presence of some common co-existing interferents such as terbutaline (TB) and tetracycline (TC), 2–aminophenol (AP), L-cysteine, folic acid (FA), uric acid (UA) with 100 folds more concentration than that of FF (0.01 µM). The developed DPV profile shown in Figure 4(d) confirms the tolerance of electrodes against these interferents. The selective response of ITO-CuO NS towards oxidation of FF is attributed to the potential selective window of 0.22 V, which may not be enough to electro-oxidize other molecules based on dissimilar charge localization in their structures. Further, the reproducibility was evaluated by fabricating five electrodes under similar experimental conditions. The response of each fabricated electrode was then assessed against 0.01 µM FF in 0.1 M BRB (pH 6.0). As seen, the variation in current response for each fabricated electrode is insignificant (<1 % RSD), reflecting the inherent signal reproducibility of ITO-CuO NS (**Fig. 4(b)**). The excellent signal reproducibility may be attributed to the identical surface morphology for analyte interaction based on an in-situ growth strategy. **Table 1** shows the analytical comparison of the proposed sensor with related works. As seen, the ITO-based CuO materials real superior analytical detection capability compared to other sensors, justifying its superiority for practical use.

The electrode was later used to quantify FF from broiler feed samples gathered from local chicken farms near Hyderabad, Pakistan. A standard addition method was considered to validate the proposed quantification technique wherein pre-spiked samples for FF were evaluated following the protocol mentioned above. Besides the excellent recoveries, few samples were noted to possess FF in very small concentrations. The obtained data are tabulated in **Table 2**, presented as **Table 2**. The excellent working performance of the ITO-CuO NS justifies its potential application to be considered an effective alternative to conventional electrochemical approaches.

Table 2. Analysis of spiked FF in three different broiler feed extract collected from various poultry farms.

Sample	Added (µM)	Determined (µM)[n]	Recovery (%)	RSD (%)
1	0.150	0.148	98.6	1.41
	0.250	0.246	98.4	1.63
	0.350	0.361	103.1	1.33
2	0.150	0.610	106.6	1.22
	0.250	0.265	106	1.54
	0.350	0.345	98.5	1.25
3	0.150	0.149	1.29	1.53
	0.250	0.230	92.0	1.22
	0.350	0.369	105.4	1.17

[n]three repetitive measurements.

Conclusion

The study reports an efficient method to synthesize/grow high-density CuO nanostructures over ITO substrate for electrochemical sensing purposes. The in-situ growth was attained, rendering a simple hydrothermal method using di-carboxylic acid (oxalic acid) taken as a potent growth moderator resulting in highly oriented, well-structured flake-like CuO nanostructures. The electrode, when tested against – adrenergic agonists such as formoterol fumarate, was capable of selective oxidation within a wide working window (0.01 µM to 0.46 µM) with a signal sensitivity of 0.001 µM. The excellent surface feature, high-contact area and identical surface morphology of the devised electrode enabled high signal reproducibility. Moreover, the excellent response of the devised electrode recorded to quantify FF from broiler feed samples further proved its working capability within practical applications. In general, the proposed route provides a simple and effective process for in-situ growth of CuO nanostructures over conductive ITO electrodes, with potential prospects for electrocatalysis and sensor applications.

Conflict of interest statement
The corresponding author states that there is no conflict of interest.

References

1. *Biol Pharm Bull,* **2006**, *29(1),* 146-9. DOI:10.1248/bpb.29.146.
2. *Journal of Chromatography B,* **2014**, *945,* 178-184. DOI: 10.1016/j.jchromb.2013.11.032.
3. *J. Chromatogr B Analyt Technol Biomed Life Sci,* **2013**, *931,*75-83. DOI: 10.1016/j.jchromb.2013.05.008.
4. *Drug Test Anal,* **2011**, *3(5),* 306-18. DOI: 10.1002/dta.258.
5. Energy Sources, Part A: Recovery, Utilization, and Environmental Effects, **2017**, *39(16),* 1815-1822. DOI: 10.1080/15567036.2017.1384866.
6. *RSC Advances,* **2015**, *5(24),* 18773-18781. DOI: 10.1039/C4RA15858J.
7. *Sensors and Actuators B: Chemical,* **2015**, *209,* 966-974. DOI: 10.1016/j.snb.2014.12.050.
8. *Microsystem Technologies,* **2015**, 1-9. DOI: 10.1007/s00542-015-2669-2.
9. *Electroanalysis,* 2002. **14**(2). 122-127 DOI:10.1002/1521-4109(200201)14:2<122::AID-ELAN122>3.0. CO;2-1.
10. *RSC Advances,* **2015**, *5(127),* 105090-105097. DOI: 10.1039/C5RA22892A.
11. *Food Chemistry,* **2016**, *190,* 544-551. DOI: 10.1016/j.foodchem.2015.05.132.
12. *Carbon,* **2016**, *98,* 90-98. DOI: 10.1016/j.carbon.2015.10.081.
13. *Journal of Materials Chemistry A,* **2016**, *4(48),* 18922-18930. DOI: 10.1039/C6TA08032D.
14. *The Journal of Physical Chemistry C,* **2015**, *119(20),* 11160-11170. DOI: 10.1021/jp5119234.
15. *Sensors and Actuators B: Chemical,* **2013**, *183,* 381-387. DOI: 10.1016/j.snb.2013.04.018.
16. *Journal of Materials Chemistry C,* 2017, *5(10),* 2708-2716 DOI: 10.1039/C6TC04611H.
17. *Journal of the American Chemical Society,* **2014**, *136(20),* 7193-7196. DOI: 10.1021/ja500197e.
18. *RSC Advances,* **2014**, *4(63),* 33446-33456. DOI: 10.1039/C4RA04214J.
19. *The Journal of Physical Chemistry C,* **2016**, *120(15),* 8323-8332. DOI: 10.1021/acs.jpcc.6b00290.
20. *Current Nanoscience,* **2009**, *5(3),* 312-317. DOI: 10.2174/157341309788921372.
21. *Inorganic Chemistry Communications,* **2017**, *86,* 213-217. DOI: 10.1016/j.inoche.2017.10.022.